Toward quantitative estimation of material properties with dynamic mode atomic force microscopy: a comparative study

IOP Publishing Nanotechnology
Nanotechnology 28 (2017) 325703 (11pp) https://doi.org/10.1088/1361-6528/aa7079

Toward quantitative estimation of material properties with dynamic mode atomic force microscopy: a comparative study

Sayan Ghosal[1,3], **Anil Gannepalli**[2] **and Murti Salapaka**[1]

[1] Department of Electrical and Computer Engineering, University of Minnesota, Minneapolis, MN, United States of America
[2] Oxford Instruments Asylum Research, Santa Barbara, California, United States of America

E-mail: ghos0087@umn.edu, Anil.Gannepalli@oxinst.com and murtis@umn.edu

Received 30 January 2017, revised 19 April 2017
Accepted for publication 2 May 2017
Published 19 July 2017

Abstract

In this article, we explore methods that enable estimation of material properties with the dynamic mode atomic force microscopy suitable for soft matter investigation. The article presents the viewpoint of casting the system, comprising of a flexure probe interacting with the sample, as an equivalent cantilever system and compares a steady-state analysis based method with a recursive estimation technique for determining the parameters of the equivalent cantilever system in real time. The steady-state analysis of the equivalent cantilever model, which has been implicitly assumed in studies on material property determination, is validated analytically and experimentally. We show that the steady-state based technique yields results that quantitatively agree with the recursive method in the domain of its validity. The steady-state technique is considerably simpler to implement, however, slower compared to the recursive technique. The parameters of the equivalent system are utilized to interpret storage and dissipative properties of the sample. Finally, the article identifies key pitfalls that need to be avoided toward the quantitative estimation of material properties.

Keywords: atomic force microscopy, nanotechnology, material characterization, signals and systems

(Some figures may appear in colour only in the online journal)

1. Introduction

Atomic force microscopy (AFM) has made significant advances in the area of nanomechanical characterization of materials. Recently a number of AFM techniques were devised for quantitative estimation of nanomechanical material properties. The principal techniques for flexure probe based mechanical property characterization can be categorized under contact mode [1, 2], cantilever resonance based dynamic mode methods [3–5] and hybrid modes based on contact resonance [6–8].

Dynamic mode methods [9] have the advantage of speed, sensitivity and minimal wear and tear over contact mode methods. However, interpretation of data is more complex for the dynamic mode in contrast to the contact mode. In resonance based techniques, quantitative estimation of the viscoelastic nature of the mechanical properties necessitates the separation of the tip-sample interaction forces into their constituent dissipative and conservative components. In a recently reported dynamic mode approach [4, 10], this separation is achieved by representing the dynamics of the cantilever interacting with the sample as an equivalent cantilever, which can be modeled as a spring mass damper (SMD) system. The resonant frequency and quality factor of the equivalent cantilever then, would depend on the viscoelastic properties of the sample. Consequently, changes in the resonant frequency and quality factors can be used to

[3] Author to whom any correspondence should be addressed.

determine the storage and loss modulus of the sample, respectively (see, for example, [11]).

In [4, 10] the cantilever is forced with a sum of three sinusoids with the primary sinusoid at or near the resonant frequency of the cantilever and the other two frequencies are chosen on either side of the center frequency. The high speed deflection response of the cantilever is analyzed digitally using a discrete time recursive estimation technique to calculate the model parameters of the equivalent cantilever. Henceforth this method will be referred to as recursive estimation (RE) method.

Alternatively the steady-state phase and amplitude of the interacting cantilever provide an estimate of the equivalent resonant frequency [11]. In this article, the steady-state phase and amplitude of the interacting cantilever are used to arrive at an estimate of the quality factor as well. As shown later in the results, this method requires the equivalent cantilever system to be in steady state and therefore, will be referred to as a steady-state estimation (SE) technique.

In this article we present analytical methods for estimating the equivalent parameters using the steady-state estimation technique and compare its performances with the recursive method. The conservative and dissipative components due to tip-sample interactions are also estimated utilizing the developed analytical methods. The newly developed results, when compared with hitherto independent approaches, validate the equivalent cantilever perspective. Another contribution of this article is a systematic study of the relative advantages of various methods available for characterizing equivalent cantilever parameters and, storage and dissipation powers of the sample for the dynamic mode AFM operation. A conclusion drawn from this study is that the different approaches yield similar results, although, care has to be taken on how the methods are executed in practice. Extensive experimental results are presented which corroborate the analytical development and conclusions.

This article is organized as the follows. In section 2 the equivalent cantilever model method is introduced, a simple semi-analytical method is derived which is applicable when the cantilever is in steady-state and a description of the recursive method for estimating the equivalent parameters is outlined. In section 3, we provide conditions and quantify differences for the estimates of the storage and dissipative powers obtained using different methods. Section 4 explains the results in detail. Section 5 concludes with the future directions of this work.

2. Equivalent cantilever system

It is well established that a freely oscillating cantilever away from the sample can be modeled as a spring mass-damper (SMD) system. The dynamics of such a system is governed by:

$$\ddot{p} + \frac{\omega_r}{Q_r}\dot{p} + \omega_r^2 p = F(t) = g(t) + h(t),$$
$$h(t) = \phi(p, \dot{p}), \quad y = p + \zeta, \tag{1}$$

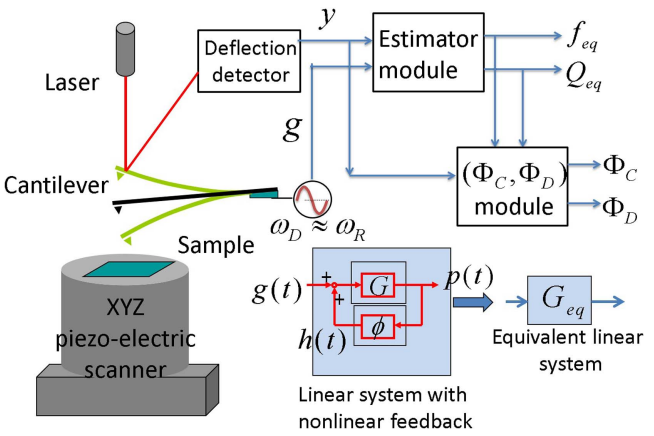

Figure 1. Estimation of storage and dissipation properties of the sample based on identifying equivalent parameters. The system including cantilever and tip-sample interaction in the dynamic mode operation is modeled with an equivalent cantilever model which is described by parameters (ω_{eq}, Q_{eq}) with $f_{eq} = \omega_{eq}/2\pi$ as shown in the figure. The equivalent parameters (f_{eq}, Q_{eq}) are further utilized for estimating average storage and dissipative power components (Φ_C, Φ_D) due to tip-sample interactive force $h = \phi(p, \dot{p})$.

where p and $\dot{p}$ are the position (or deflection) and velocity of the cantilever-tip respectively. F is the force per unit mass on the cantilever, F equals the sum of the excitation force, g, and the non-linear tip-sample interaction force, h. The measured position, y, is the position corrupted with measurement noise, ζ. ω_r and Q_r are the natural resonant frequency and quality factor of the cantilever at the reference position far from the sample where the tip-sample interaction forces are non-existent or negligible. From a systems perspective, the cantilever interacting with the sample can then be represented as a cantilever G with parameters (ω_r, Q_r) in feedback with the non-linear tip-sample forcing term h, as shown in figure 1.

The systems viewpoint presented above and tools from asymptotic methods for weakly non-linear systems [12, 13] can be used to model a cantilever being driven at or near resonance and interacting with the sample periodically, as an SMD described by [14, 15]:

$$\ddot{p} + \frac{\omega_{eq}(a)}{Q_{eq}(a)}\dot{p} + \omega_{eq}^2(a)p = g(t) = \sin(\omega_d t), \tag{2}$$

where ω_{eq} and Q_{eq} are the resonant frequency and quality factor of the equivalent cantilever system G_{eq}, and a denotes the amplitude of cantilever oscillations. $\omega_d \approx \omega_r$ is the drive frequency forcing the cantilever. The parameters (ω_{eq}, Q_{eq}) of the equivalent cantilever, or equivalent parameters in short, can be estimated using the methods described below. Also, note that the equivalent parameters ω_{eq} and Q_{eq} depend on the amplitude a which is slowly varying in comparison to the forcing time-period, $\frac{2\pi}{\omega_d}$ (see [14]).

2.1. Steady-state estimation of equivalent parameters (SE)

In a recent study [11], the equivalent cantilever approach was employed to determine the equivalent stiffness using the amplitude and phase of the cantilever oscillations in dynamic

mode. Thus the amplitude and phase information can be used to estimate the equivalent resonant frequency.

Here we extend the approach in [11] to determine the equivalent quality factor as well. Let a_r and a denote the oscillation amplitude of the cantilever at the reference position and when interacting with sample respectively. Using (1) and (2), the ratio of the amplitudes can be shown to be:

$$\frac{a_r}{a} = \sqrt{\frac{(\omega_{eq}^2 - \omega_d^2)^2 + \omega_d^2\omega_{eq}^2/Q_{eq}^2}{(\omega_r^2 - \omega_d^2)^2 + \omega_d^2\omega_r^2/Q_r^2}}. \tag{3}$$

The phase of the cantilever oscillations, with respect to the drive signal, at the reference position and when interacting with the sample are given by:

$$\theta_r = \arctan\left(\frac{\omega_d\omega_r}{Q_r(\omega_r^2 - \omega_d^2)}\right)$$

and

$$\theta = \arctan\left(\frac{\omega_d\omega_{eq}}{Q_{eq}(\omega_{eq}^2 - \omega_d^2)}\right), \tag{4}$$

respectively. We can rewrite (3) as:

$$\frac{a_r}{a} = \frac{(\omega_{eq}^2 - \omega_d^2)}{\omega_d^2\omega_r^2/Q_r}\sqrt{\frac{\frac{\omega_d^2\omega_{eq}^2}{Q_{eq}^2(\omega_{eq}^2 - \omega_d^2)} + 1}{\frac{(\omega_r^2 - \omega_d^2)^2Q_r^2}{\omega_d^2\omega_r^2} + 1}}. \tag{5}$$

Using (4) with the trigonometric identities $\sec^2 x = \tan^2 x + 1$; $\csc^2 x = \cot^2 x + 1$, (5) reduces to

$$\frac{a_r}{a} = \frac{(\omega_{eq}^2 - \omega_d^2)\sin\theta_r}{\omega_d^2\omega_r^2\cos\theta/Q_r}. \tag{6}$$

Rearranging the expression above, the equivalent resonant frequency can be obtained as:

$$\omega_{eq} = \omega_r\sqrt{\frac{\omega_d^2}{\omega_r^2} + \frac{a_r\omega_d\cos\theta}{Q_r a\omega_r\sin\theta_r}}. \tag{7}$$

Similarly, by recomposing (3) as

$$\frac{a_r}{a} = \frac{\omega_d^2\omega_r^2/Q_{eq}}{\omega_d^2\omega_r^2/Q_r}\sqrt{\frac{\frac{(\omega_{eq}^2 - \omega_d^2)^2Q_{eq}^2}{\omega_d^2\omega_{eq}^2} + 1}{\frac{(\omega_r^2 - \omega_d^2)^2Q_r^2}{\omega_d^2\omega_r^2} + 1}}, \tag{8}$$

we can express the equivalent quality factor:

$$Q_{eq} = Q_r\frac{a\omega_{eq}\sin\theta_r}{a_r\omega_r\sin\theta}. \tag{9}$$

Both a and θ are available in real time in standard dynamic mode AFM operation. (ω_r, Q_r), a_r and θ_r can be experimentally determined from a cantilever's frequency response at the reference position. $f_{eq} = \omega_{eq}/2\pi$ and Q_{eq} determined using (7) and (9) are referred to as f_{SE} and Q_{SE} respectively.

2.2. Discrete time recursive estimation of equivalent parameters (RE)

The continuous-time second order system in (2) can be discretized by a general second order discrete time system [10] described by:

$$\begin{aligned} p(k) &= -b_1p(k-1) - b_0p(k-2) + u(k) + e(k),\\ u(k) &= a_2g(k) + a_1g(k-1) + a_0g(k-2),\\ e(k) &= \zeta(k) + b_1\zeta(k-1) + b_0\zeta(k-2), \end{aligned} \tag{10}$$

where $p(k)$ and $g(k)$ denote the cantilever deflection and driving force sampled at time $t = kT_s$, T_s being the sampling interval. Here, $\zeta(k)$ is zero mean white measurement noise. The unknown parameters can be recursively estimated using a least square approach by defining the model parameter vector $m = \begin{bmatrix} b_1 & b_0 & a_0 & a_1 & a_2 \end{bmatrix}$, the observation vector $\psi(k)$

$= \begin{bmatrix} -p(k-1) & -p(k-1) & g(k) & g(k-1) & g(k-2) \end{bmatrix}^T$ and noticing that $p(k) = m\psi(k) + e(k)$. However, it is seen that (a_2, a_1, a_0) can be evaluated from the discrete time equivalent of the dynamics of the cantilever at the reference position (which is estimated by applying a frequency sweep method around first resonant frequency). Subsequently the values of a_2, a_1 and a_0 can be fixed to the reference values which leads to a simpler parameter identification problem [10]. Thus (10) can be simplified as

$$\gamma(k) = \underbrace{[b_1 b_0]}_{\Gamma^T}\underbrace{\begin{bmatrix} -p(k-1) \\ -p(k-2) \end{bmatrix}}_{\phi(k)} + e(k), \tag{11}$$

where $\gamma(k) = p(k) - a_2g(k) - a_1g(k-1) - a_0g(k-2)$. A recursive least square estimate of Γ denoted as $\hat{\Gamma}(k) = \begin{bmatrix} \hat{b}_1 & \hat{b}_0 \end{bmatrix}^T$ can be used to determine the equivalent parameters ω_{eq} and Q_{eq} in closed form [10]. The equivalent parameters estimated by the recursive method will be denoted by f_{RE} $(=\omega_{RE}/2\pi)$ and Q_{RE}.

3. Storage and dissipative powers of the equivalent system

The time averaged power dissipated by the cantilever per oscillation cycle, denoted by Φ_D, is defined as $\Phi_D = -\frac{1}{T}\int_0^T \phi(p, \dot{p})\dot{p}\, dt$. Similarly, the time averaged storage power, denoted by Φ_C, attributed to tip-sample interaction is $\Phi_C = \frac{\omega_d}{T}\int_0^T \phi(p, \dot{p})p\, dt$. It follows from averaging theory [4, 16] that the dissipation and storage powers are related to the equivalent parameters by:

$$\Phi_D = \frac{ma^2\omega_d^2}{2}\left(\frac{\omega_{eq}}{Q_{eq}} - \frac{\omega_r}{Q_r}\right) \text{ and,} \tag{12}$$

$$\Phi_C = \frac{ma^2\omega_d}{2}(\omega_r^2 - \omega_{eq}^2), \tag{13}$$

respectively, where m is the mass of the cantilever. Substituting expressions for ω_{eq} and Q_{eq} from (7) and (9), and recognizing that the cantilever mass m is related to the cantilever stiffness k by $k = m\omega_r^2$, it follows that,

$$\Phi_D = \frac{ka^2\omega_d}{2Q_r}\left(\frac{a_r\omega_d\sin\theta}{a\omega_r\sin\theta_r} - \frac{\omega_d}{\omega_r}\right) \tag{14}$$

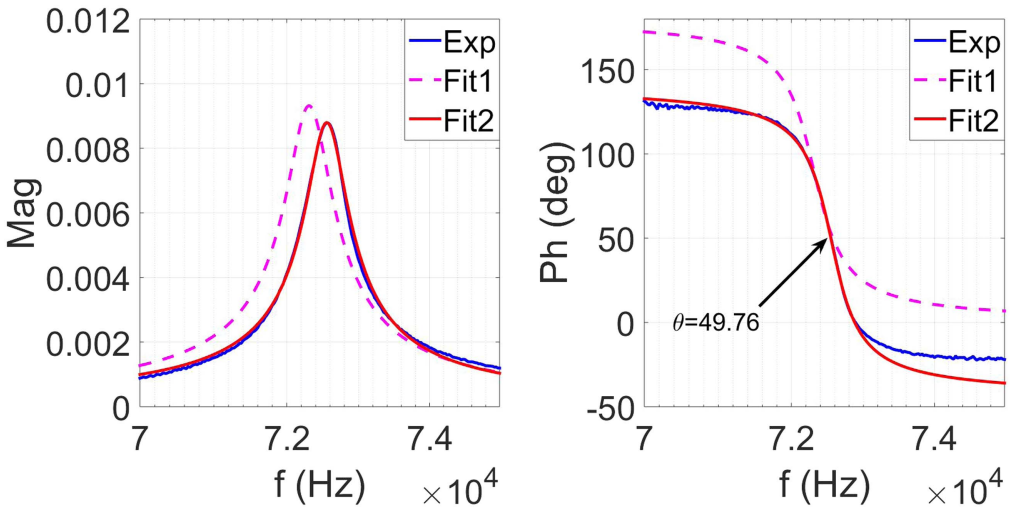

Figure 2. (Experimental data) Frequency response of cantilever in free air. Data is fit using a plant model with $\alpha_1 = 0$ denoted by Fit 1. Fit 2 is obtained using nonzero α_1. Fit 2 better approximates the frequency response.

and

$$\Phi_C = \frac{kaa_r\omega_d}{2Q_r}\left(\frac{aQ_r}{a_r}\left(1 - \frac{\omega_d^2}{\omega_r^2}\right) - \frac{\omega_d \cos\theta}{\omega_r \sin\theta_r}\right). \tag{15}$$

Alternatively, the average dissipation power due to tip-sample interaction can be evaluated using energy conservation principles [17]. The dissipation power derived by energy conservation, denoted by P_D, can be expressed as [17]:

$$P_D = \frac{ka^2\omega_d}{2Q_r}\left(\frac{a_r}{a}\sin\theta - \frac{\omega_d}{\omega_r}\right). \tag{16}$$

Using the virial theorem, the average storage power, denoted by P_C, can be derived as [3, 18]:

$$P_C = \frac{kaa_r\omega_d}{2Q_r}\left(\frac{aQ_r}{a_r}\left(1 - \frac{\omega_d^2}{\omega_r^2}\right) - \cos\theta\right). \tag{17}$$

Comparing (14)–(15) with (16)–(17) it can be observed that $\Phi_D = P_D$ and $\Phi_C = P_C$ when

$$\frac{\omega_d}{\omega_r \sin\theta_r} = 1. \tag{18}$$

Using (4) and the identity $\sin^2\theta_r = \tan^2\theta_r/(\tan^2\theta_r + 1)$ the above condition (18) can be written as

$$\left(Q_r^2\left(1 - \frac{\omega_d^2}{\omega_r^2}\right) - 1\right)\left(1 - \frac{\omega_d^2}{\omega_r^2}\right) = 0, \tag{19}$$

which has two solutions:

$$\omega_d = \omega_r, \text{ and}$$
$$\omega_d = \omega_r\sqrt{1 - \frac{1}{Q_r^2}}. \tag{20}$$

This equivalence of $\Phi_D = P_D$ and $\Phi_C = P_C$ is an important result and, to the best of our knowledge, the first study that validates the steady state estimation of the parameters of the equivalent model. Furthermore, the above result not only reiterates the aforementioned assumption requiring ω_d to be at or near ω_r, but also quantifies the magnitude of error for a given choice of ω_d. This can be used to calculate the error bounds for quantitative results based on the equivalent model approach.

4. Results and discussions

Let u denote the drive signal to the dither piezo at the base of the cantilever. We observed from experiments that a transfer function of the form,

$$G_r(s) = \frac{\alpha_1 s + \alpha_2}{s^2 + \frac{\omega_r}{Q_r}s + \omega_r^2}, \tag{21}$$

explains the cantilever dynamics from the drive u to the measured tip-deflection y_m. Here the numerator contains a non zero coefficient α_1 of s. Under the assumption of ideal SMD model, α_1 would be zero. The rationale for choosing (21) to represent the dynamics of the cantilever is provided below.

Frequency response of AC240TS cantilever from Asylum Research obtained by applying frequency sweep input in free air is shown in figure 2. The peak frequency $f_p = \omega_p/2\pi$ is found to be 72.55 kHz with the phase $\theta = 49.76$ degrees. The frequency response is fit with plant model first described by $\alpha_1 = 0$ in (21) (called Fit 1) followed by nonzero α_1 (called Fit 2). For Fit 2, The departure of the phase θ from 90 degrees at resonant peak can be shown to be equal to $\theta_c = \arctan(\alpha_1\omega_p/\alpha_2)$. It is evident from figure 2 that Fit 2 ($\alpha_1 \neq 0$) not only better fits the frequency response data than Fit 1 ($\alpha_1 = 0$), it also explains the departure of phase from 90 degrees at f_p (40.24 degrees from figure 2) which is close to $\theta_c = \arctan(\alpha_1\omega_p/\alpha_2) = 41.93$ degrees. Repeated experiments confirm the same conclusion.

Due to $\alpha_1 \neq 0$, the analytical formulas for equivalent parameters and storage-dissipative powers shown in section 2 and section 3 must be adjusted to accommodate for the non-ideal SMD behavior. Using similar steps outlined in sections 2 and 3, it can be shown that the phase terms θ and θ_r in (7), (9), (14), (15), (16), (17), and (18) should be replaced

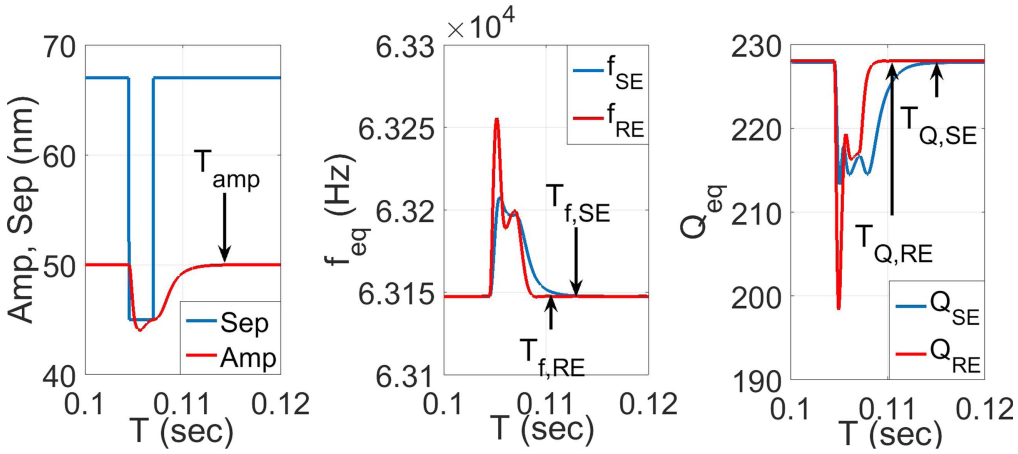

Figure 3. (Simulation data) Equivalent parameters ($f_{eq} = \omega_{eq}/2\pi$, Q_{eq}) estimated using steady-state and recursive techniques during transient and steady-state part of the trajectory of an oscillating cantilever. When *sep* is low (high), the oscillating cantilever interacts (does not interact) with the sample. In absence of a sample, the cantilever is described by ideal SMD with resonant frequency $f_r = \omega_r/2\pi = 63.15$ kHz and quality factor $Q_r = 227.9$.

with $\tilde{\theta} := \theta + \theta_c$ and $\tilde{\theta}_r := \theta_r + \theta_c$ respectively where θ_c acts as a phase offset. θ_c can be estimated using the frequency response of the cantilever at the reference position as described above and subsequently added to θ and θ_r. This step is termed as the: phase offset correction.

The main contributing factor for the numerator polynomial being first order and not a constant in G_r is hypothesized as being caused by the presence of delays between the drive and the tip-deflection which include both electronic and structural effects. In this article we leave the study of the sources of the delays to future work; here it is assumed that the transfer functions from the drive to the tip-deflection measurement when intermittently interacting with the sample and at the reference position share the same numerator polynomial.

4.1. Speed of real-time estimation

Here we first present a comparison of the steady-state method and the recursive technique of estimating the equivalent parameters during transient and steady-state part of cantilever oscillations using simulation. The interactive forces between the sample and tip of the cantilever in air typically follows a long range attractive and short range repulsive behavior. This behavior is modeled with a piecewise linear model which consists of two springs and two dampers shown in [15, 19] which we utilize for simulation. Such a model is useful to mimic interactive forces from many substrates in air [14, 15].

A cantilever with resonant frequency $f_r = \omega_r/2\pi = 63.15$ kHz and quality factor $Q_r = 227.9$ at the reference position is driven at the resonant frequency, that is $\omega_d = \omega_r$ such that the amplitude of oscillation is 50 nm. The distance between the cantilever base and the sample (shown as *sep* in figure 3) is varied in a step wise fashion such that when *sep* is low (high), the oscillating cantilever interacts (does not interact) with the sample. Such steps in *sep* periodically nudges the oscillating cantilever away from its steady state so that transient behavior of oscillations can be observed. Figure 3 shows the transient response from the cantilever.

$f_{eq} = \omega_{eq}/2\pi$ and Q_{eq} estimated using the steady-state method are denoted as f_{SE} and Q_{SE} respectively. Further, f_{RE} and Q_{RE} denote the corresponding parameters estimated using recursive method. The measurement bandwidth and noise in the estimates f_{SE} and Q_{SE} depend on the bandwidth of the lock-in filter which is utilized to gather the amplitude, a and phase signal, θ from cantilever deflections. The measurement bandwidth and noise variance in the recursive estimates depend on the choice of forgetting factor [10] and bandwidth of the low pass filters that are utilized to reduce the noise contents in f_{RE} and Q_{RE}. For comparison, the bandwidth of a lock-in filter in steady-state technique, the forgetting factor and bandwidth of low pass filters in recursive technique are chosen such that the noise in both steady-state and recursive estimates are the same in a steady state. Although reducing the low pass bandwidth of the lock-in filter reduces the noise in steady-state method, the bandwidth is kept high enough so that the time constants of the estimated amplitude, a, of the cantilever oscillations are not influenced by the lock-in filter.

When the oscillating cantilever transitions from the interaction state (*sep* is low) to no-interaction state (*sep* is high), the time to attain a steady state for the parameters $f_{eq} = \omega_{eq}/2\pi$ and Q_{eq} estimated using recursive and steady-state methods is observed in figure 3. Both recursive and steady-state methods match when the cantilever reaches steady-state oscillations (see figure 3). In figure 3, T_{amp} denotes the time required to reach steady state by the amplitude of cantilever oscillations. $T_{f,RE}$ and $T_{Q,RE}$ denote the convergence times for equivalent frequency and quality factors estimated using the recursive technique. Similarly, $T_{f,SE}$ and $T_{Q,SE}$ represent corresponding convergence times for the steady-state method (see figure 3). It is observed that the estimates using recursive method converge faster than the steady-state technique. For this example, steady-state method requires 9.5 ms so that both of f_{SE} and Q_{SE} attain convergence (from the beginning of the sudden interaction). However, f_{RE}

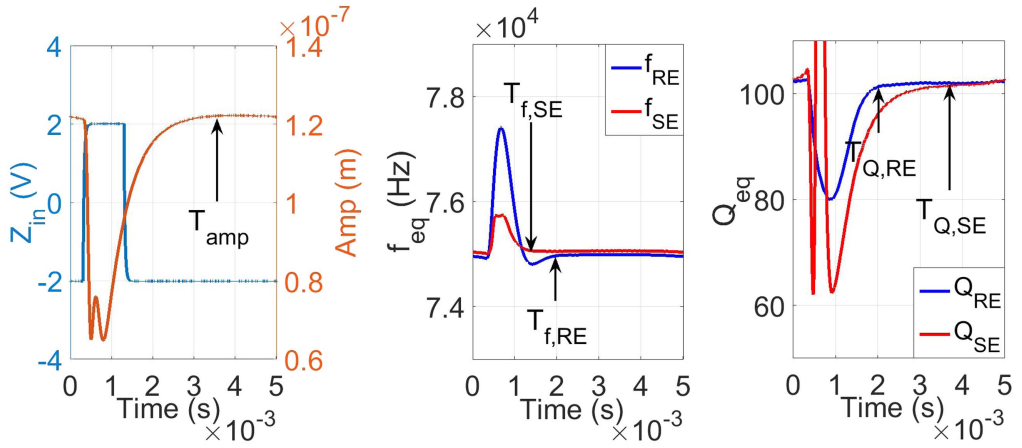

Figure 4. (Experimental data) (a) The input signal Z_{in} (in V) to z-piezo actuator with amplitude of cantilever oscillations *Amp* (in meter). (b) Estimated equivalent frequencies (in Hz). (c) Estimated equivalent quality factors. Time axis is in seconds.

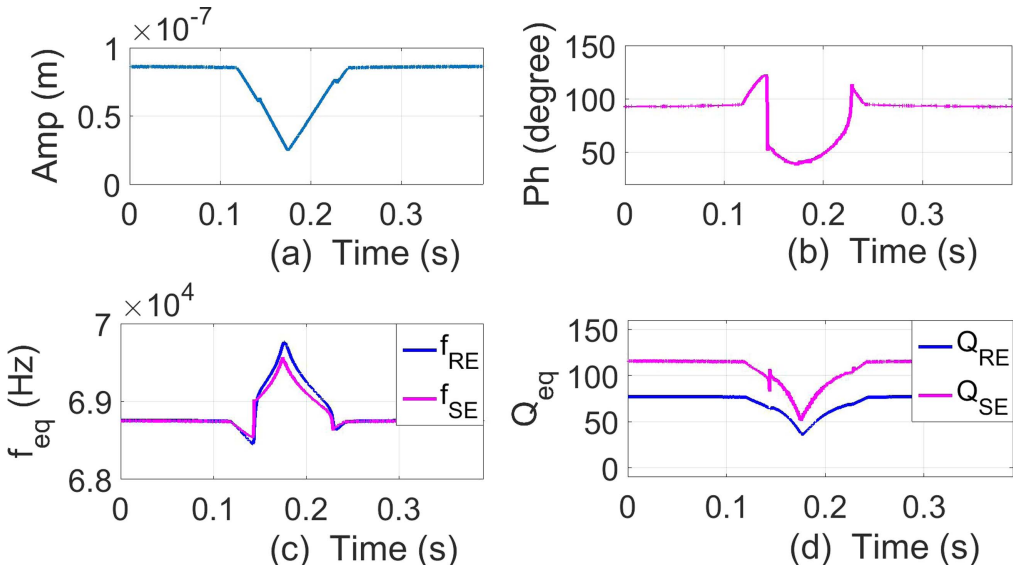

Figure 5. (Experimental data) (a) Deflection amplitude a (meter) during approach-retract cycle on freshly cleaved mica. (b) Offset corrected phase $\tilde{\theta}$ (degrees). (c) Equivalent frequency using recursive (f_{RE}) and steady-state method (f_{SE}) in Hz. (d) Equivalent quality factor using recursive (Q_{RE}) and by steady-state method (Q_{SE}). The reference position is chosen in free air. Time axis is in seconds.

and Q_{RE} converge near 5.8 ms which is about 39% smaller than the time required by steady-state estimation. Though the exact convergence times may vary from one example to another, recursive estimation is consistently observed to be faster than steady-state estimation.

We now present experimental results below. The cantilever is driven sinusoidally near mica substrate such that it oscillates with an oscillation amplitude of 122 nm. The parameters at reference position $f_r = \omega_r/2\pi$ and Q_r are found using frequency sweep method which are 73.4 kHz and 131.6 respectively. The mica substrate is actuated in the z-direction using a piezoelectric actuator. A pulse waveform (shown as Z_{in} in figure 4(a)) is applied to the piezoelectric actuator such that the mica substrate periodically nudges the oscillating cantilever out of its steady state. Both recursive and steady-state methods are employed to estimate the equivalent parameters which are shown in the figure 4. In figure 4(a), it is observed that after the nudge arrives, the oscillation amplitude takes $T_{amp} = 3.4$ ms to recover to its steady state value of 122 nm. It should be noted that the bandwidth of oscillation amplitude of the cantilever is given by $f_B = f_r/(2Q_r) = 73.4\,\text{kHz}/131.6 = 279\,\text{Hz}$. Thus the expected recovery time $t_B = 1/f_B = 3.6$ ms is consistent with the observation $T_{amp} = 3.4$ ms. From figures 4(b) and (c), the time to reach steady state for estimates f_{SE} and Q_{SE} are observed to be $T_{f,SE} = 1.4$ ms and $T_{Q,SE} = 3.5$ ms respectively. Thus, interpretation of data is possible after 3.5 ms which is close to the recovery time of amplitude ($T_{amp} = 3.4$ ms). From figures 4(b) and (c), the times to attain a steady state for f_{RE} and Q_{RE} (denoted by $T_{f,RE}$ and $T_{Q,RE}$ respectively) are both 1.8 ms. Indeed, recursive estimation offers superior bandwidth than the steady-state method. It is evident from figure 4 that both the recursive and steady-state methods yield estimates that agree with each other when the cantilever oscillation reaches steady state.

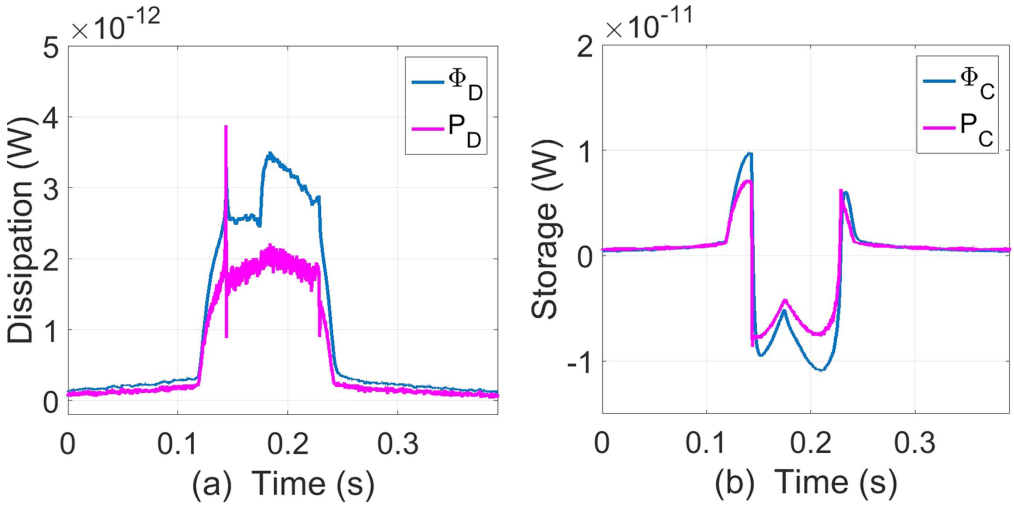

Figure 6. (Experimental data) (a) Dissipation power using recursive estimation technique (Φ_D) and by (16) shown as P_D (unit watt). (b) Storage power Φ_C estimated using recursive method and using (17) which is denoted as P_C (in watt). The reference position is chosen in free air. Time axis is in seconds.

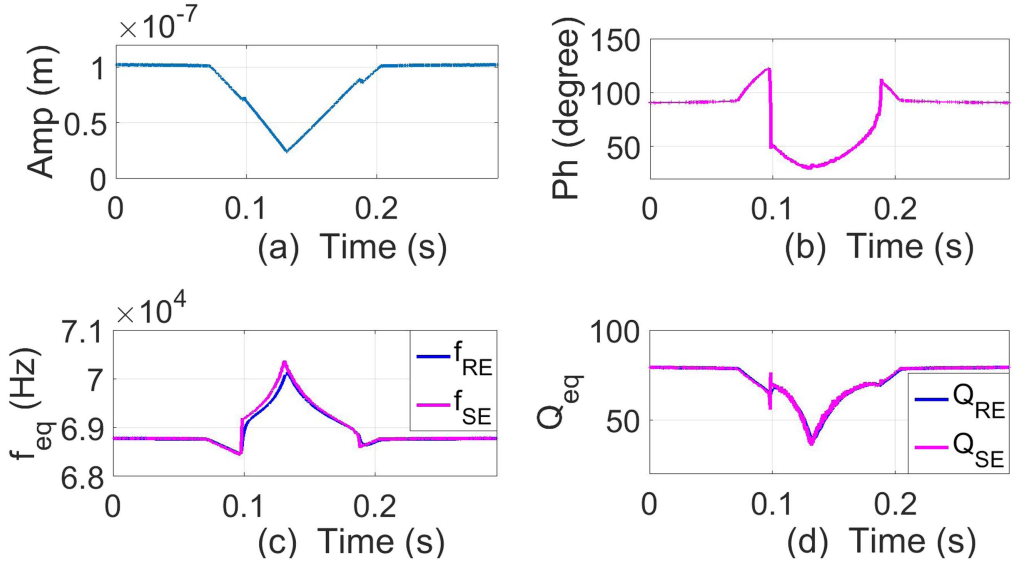

Figure 7. (Experimental data) (a) Oscillation amplitude a (meter) (b) Offset corrected phase $\tilde{\theta}$ (degrees). (c) Equivalent frequency using recursive (f_{RE}) and steady-state method (f_{SE}) in Hz. (d) Equivalent quality factor using recursive (Q_{RE}) and steady-state method (Q_{SE}). The reference position is chosen near the sample to include squeeze film damping. Time axis is in seconds.

4.2. Approach-retract experiments on mica

Dynamic mode force curve (approach-retract) experiments are performed on a freshly cleaved mica sheet using MFP-3D AFM from Asylum Research. Such approach-retract cycles are sufficiently slow so that the cantilever oscillation can be assumed to be in steady-state. It should be noted that closer to the sample surface, changes in the effective damping result which are attributed to squeeze film damping effects (see [17]) where the non-linear interactions between the cantilever-tip and sample, denoted as h in (1), is still negligible ($h \approx 0$). Care must be taken to include the effect of squeeze film damping while selecting the reference position for cantilever model. We first demonstrate the need for choosing a proper reference position.

The free-air cantilever transfer function model from dither excitation signal u to the measured deflection y_m is estimated using a frequency sweep method [20]. The first mode resonant frequency and quality factor are found as $f_r = \omega_r/2\pi = 68.765$ kHz and $Q_r = 116.287$. The numerator coefficients of the transfer function as shown in (21) in free-air are estimated to be $\alpha_1 = 5.6526e + 03$ and $\alpha_2 = -3.3618e + 06$. The excitation and deflection data of the cantilever are gathered with sampling frequency of 1.024 MHz. Recursive method based estimates are denoted by f_{RE} and Q_{RE}. The drive frequency f_d ($=\omega_d/2\pi$) is the same as f_r (68.765 kHz). The reference oscillation amplitude (same as free air amplitude) is set to be $a_r = 125.26$ nm. $f_{SE} = \omega_{SE}/2\pi$ and Q_{SE} are determined using (7) and (9) with offset corrected phase terms, $\tilde{\theta}$ and $\tilde{\theta}_r$. Figure 5 suggests that

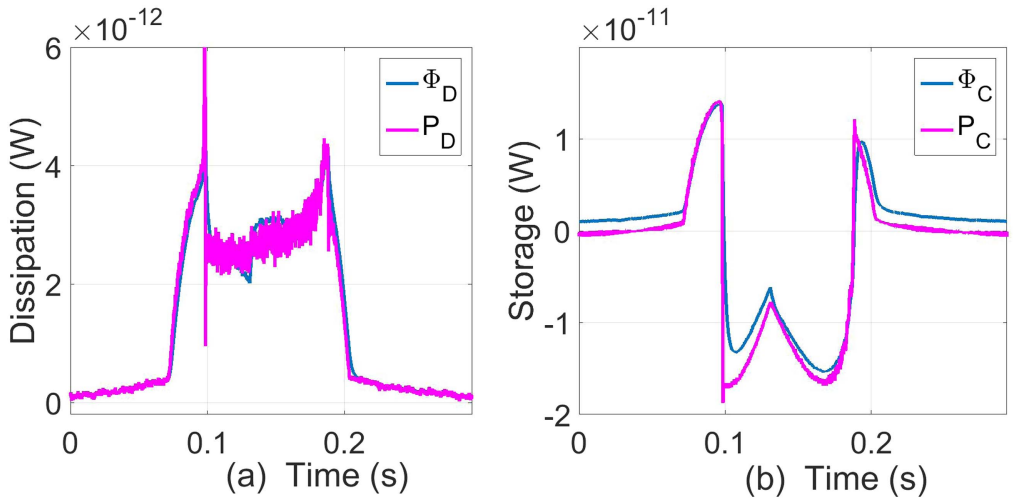

Figure 8. (Experimental data) (a) Dissipation power using recursive technique (Φ_D) and P_D using (16) (in watt). (b) Storage power using a recursive estimation technique (shown as Φ_C) and using (17) denoted as P_C (in watt). The reference position is chosen near sample to include the squeeze film damping effect. Time axis is in seconds.

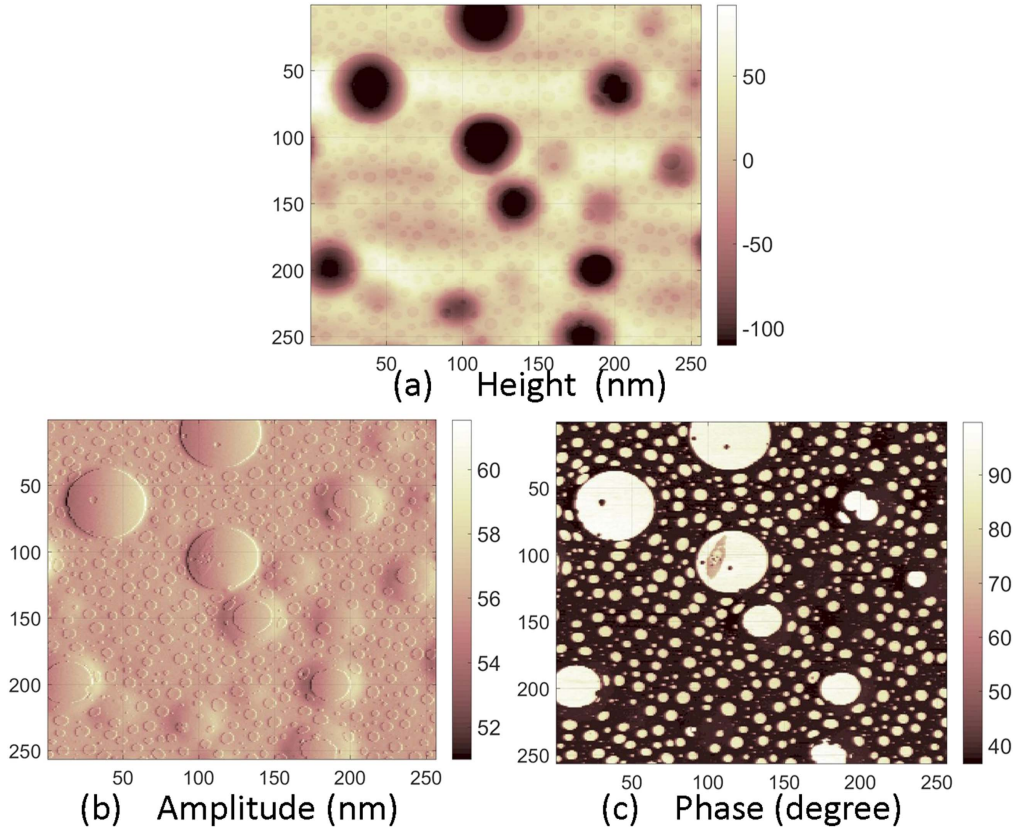

Figure 9. (Experimental data) (a) Height image (nm), (b) amplitude image (nm) and (b) $\tilde{\theta}$ phase image (degrees) of a 20 μm × 20 μm PLMA-PBMA polymer sample.

estimated frequencies f_{RE} and f_{SE} match well. However Q_{RE} and Q_{SE} deviate considerably from each other. In figure 5(d), the average percentage difference between Q_{RE} and Q_{SE} is 33.6%. This discrepancy is attributed to inappropriate choice of reference position which in this case is the free-air model. The storage power Φ_C and dissipation power Φ_D are evaluated as described in section 3 using the recursive technique. Storage power P_C and dissipative power P_D are also evaluated utilizing conservation principles from (17) and (16) respectively (with offset corrected phase terms, $\tilde{\theta}$ and $\tilde{\theta}_r$) which are compared in figure 6. Evidently P_C matches with Φ_C. However Φ_D and P_D differ significantly when the oscillating cantilever engages with the sample. In figure 6(a), the average percentage error between Φ_D and P_D is 72.3%. Again this difference is attributed to ignoring the effect of squeeze film damping and choosing incorrect Q_r and θ_c (thus $\tilde{\theta}$).

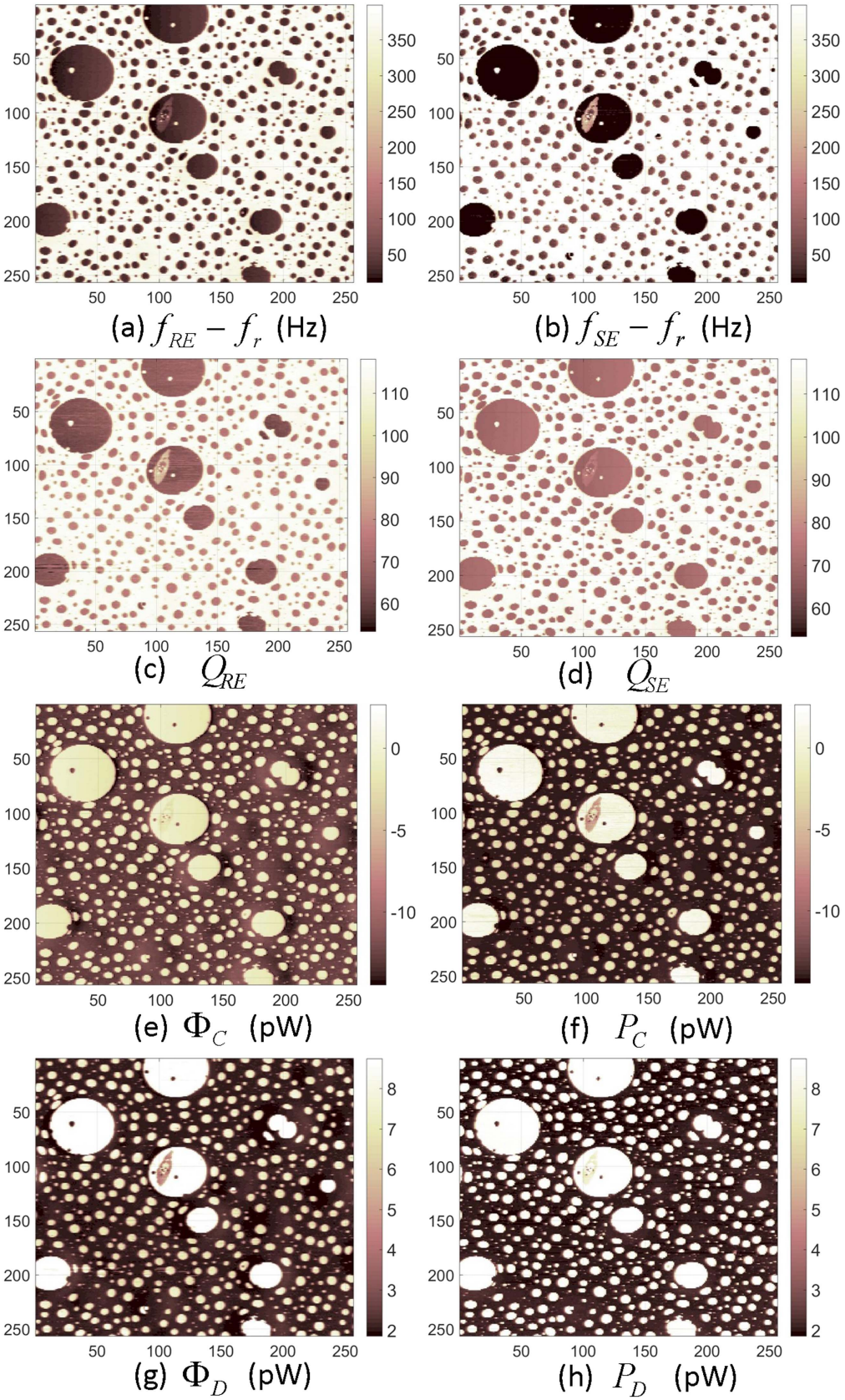

Figure 10. (Experimental data) (a) Shift of equivalent frequency of oscillating cantilever $f_{eq} - f_r$ determined through recursive estimation (f_{RE}) and (b) using steady-state estimation method (f_{SE}) in Hz where $f_r = 72.273$ kHz. (c) Equivalent quality factor evaluated using recursive technique (Q_{RE}) and (d) using steady-state method (Q_{SE}). (e) Storage power Φ_C evaluated through recursive technique and (f) P_C estimated using (17) in pW. (g) Dissipative power Φ_D estimated by recursive method and (h) P_D estimated using (16) in pW.

Now the cantilever transfer function is estimated using a frequency chirp at a reference position which is close to the sample to include squeeze film damping. The reference parameters are found to be $f_r = \omega_r/2\pi = 68.857$ kHz and $Q_r = 74.61$ with the numerator coefficients $\alpha_1 = 4.455e + 03$, $\alpha_2 = 7.9461e + 08$. $f_d = \omega_d/2\pi$ is chosen as 68.784 kHz. Amplitude of oscillations at reference a_r is chosen to be 102.67 nm. (f_{SE}, Q_{SE}) are determined using (7) and (9). Discretizing the transfer function at reference position yields the parameters (a_2, a_1, a_0) which are used by the recursive estimation method. From figures 7(c) and (d), the close match of f_{RE} with f_{SE} and Q_{RE} with Q_{SE} can be observed. The difference between Q_{RE} and Q_{SE} from figure 7(d) is estimated to be 0.94% which is much smaller compared to 33.6% in figure 5(d). Further, the percentage difference between Φ_D and P_D from figure 8(a) is determined to be 13% in contrast to 72.3% observed in figure 6(a). The storage power Φ_C determined through recursive technique and P_C estimated using (17) also match closely in figure 8(b). Thus, selection of a proper reference position plays an important role in determining the storage and dissipative parameters.

4.3. Imaging PLMA-PBMA polymer sample

The equivalent model allows us to interpret properties of the sample by processing the trajectory of the cantilever. For example, while maintaining the same set point amplitude of oscillations, a, if the equivalent model has higher resonant frequency, ω_{eq}, on some areas of the sample compared to other locations, then those areas of the sample can be interpreted to be mechanically stiffer [4] than the other locations.

A real time algorithm for recursive estimation is designed and implemented on Xilinx ML605 FPGA kit. After extensive verification of the developed FPGA design through simulations and experiments, the design is used to process dither excitation u and measured deflection y_m from MFP-3D AFM to estimate the equivalent parameters f_{RE} and Q_{RE} in real time. Dynamic mode imaging is performed on a blend of poly-lauryl methacrylate (PLMA) and poly-butyl methacrylate (PBMA) sample.

AC240TS cantilever with free-air resonant frequency $f_0 = 72.7$ kHz and quality factor $Q_0 = 146.4$ is selected for imaging. The reference position is chosen near the sample and the frequency tune near first mode resonance is used to estimate (α_1, α_2) and the bias phase θ_c is as explained previously. This offset correction for θ is also done in the Igor Pro software from Asylum Research during AC mode tuning near the sample. The dynamic mode height, phase $\tilde{\theta}$ and amplitude images of a 20 $\times$ 20 micron sample is shown in figure 9. Drive frequency f_d is chosen to be 72.738 kHz. Equivalent parameters determined both using steady-state estimation technique and recursive estimation method are shown in figure 10. Evidently, steady-state and recursive estimation for equivalent parameters (f_{eq}, Q_{eq}) provide a close match. Further, storage and dissipative power images are computed and shown in figure 10. Close similarity between estimated storage powers Φ_C and P_C is evident from figures 10(e) and (f). Dissipative power Φ_D evaluated through recursive technique and P_D using (16) are shown in figures 10(g) and (h) that are also close match.

The contrast in the surface mechanical properties of the PLMA and PBMA polymers are demonstrated in figure 10. In the polymer sample, the circular PLMA domains are distributed over the PBMA background. Figures 10(a) and (b) demonstrate that the equivalent frequency values are higher over the PBMA surface compared to the PLMA domains. Thus, PBMA is estimated to be mechanically stiffer compared to PLMA polymer. This inference is consistent with the fact that PBMA is glassy and stiffer at room temperature whereas PLMA is rubbery and softer [21]. The same conclusion can be drawn from figures 10(e) and (f) where the lower valleys in the conservative power image (Φ_C or P_C) imply stiffer domains. The dissipative power due to tip-sample interactions depends jointly on f_{eq} and Q_{eq} (observe (14)) where, typically, low Q_{eq} domains indicate higher dissipation. It can be observed in figures 10(e) and (f) that the PLMA domains are contrasted with lower Q_{eq} values compared to PBMA regions. Figures 10(g) and (h) further contrast the dissipative properties (Φ_D or P_D) where the PLMA domains are observed to be more dissipative which is consistent with the rubbery phase of PLMA in contrast to the glassy phase of PBMA at room temperature.

It is important to note, and is evident from the study on PLMA/PBMA above, that the knowledge of the equivalent parameters together with the storage and dissipation powers afford the ability to reach conclusions on the *relation* of properties of one material with respect to another. We remark that considerable work remains in reaching conclusions on material properties such as stiffness and loss modulus of a given sample where, uncertainties in the parameters assumed need to be quantified accurately. Here, for instance, the uncertainty in the stiffness of the AC240TS cantilevers is accurate within $\pm 5.1\%$ with a confidence interval of 95% that is consistent with the results obtained in [22]. However, there is still a need for methods for quantifying other sources of uncertainty and to provide measures on the impact on interpretation toward quantitative determination of material properties. Assessment of error bounds and determining confidence measures on AFM measurement data in general is a challenging problem [23, 24]. The equivalent parameter estimation is only the first, but necessary, step of any method for the quantitative determination of material properties using the equivalent cantilever system viewpoint. Sources of uncertainty are common for the two methods for determination of equivalent parameters that are compared in the study and thus their affect on the conclusions reached are mitigated.

5. Conclusion

This article compares a steady state based method with a recursive estimation technique for estimating the equivalent parameters, resonance frequency and quality factor, of an interacting cantilever in the dynamic mode operation of AFM. The method based on steady state analysis is considerably

simpler as it uses amplitude and phase signals that are readily available in dynamic mode. On the other hand, the recursive estimation technique requires complex hardware implementation and careful selection of excitation signals at multiple frequencies. However, the recursive technique is demonstrated to be valid during the transient phase of cantilever dynamics and therefore offers a higher bandwidth of estimation than the steady state method. The importance of the selection of an appropriate reference state of the tip-sample system for accurate estimation of parameters is demonstrated experimentally. The knowledge of the equivalent parameters is imperative for any technique that attempts to determine the mechanical properties of the sample using the equivalent system perspective in dynamic AFM. This study, for the first time, proves the validity of the steady state analysis of the equivalent cantilever system approach.

ORCID

Sayan Ghosal https://orcid.org/0000-0001-6878-7522

References

[1] Radmacher M, Tillmann R W and Gaub H E 1993 Imaging viscoelasticity by force modulation with the atomic force microscope *Biophys. J.* **64** 735–42
[2] Schaer-Zammaretti P and Ubbink J 2003 Imaging of lactic acid bacteria with afmelasticity and adhesion maps and their relationship to biological and structural data *Ultramicroscopy* **97** 199–208
[3] Proksch R and Yablon D G 2012 Loss tangent imaging: theory and simulations of repulsive-mode tapping atomic force microscopy *Appl. Phys. Lett.* **100** 073106
[4] Saraswat G, Agarwal P, Haugstad G and Salapaka M V 2013 Real-time probe based quantitative determination of material properties at the nanoscale *Nanotechnology* **24** 265706
[5] Garcia R and Proksch R 2013 Nanomechanical mapping of soft matter by bimodal force microscopy *Eur. Polym. J.* **49** 1897–906
[6] Nikiforov M P, Jesse S, Morozovska A N, Eliseev E A, Germinario L T and Kalinin S V 2009 Probing the temperature dependence of the mechanical properties of polymers at the nanoscale with band excitation thermal scanning probe microscopy *Nanotechnology* **20** 395709
[7] Balke N, Jesse S, Morozovska A N, Eliseev E, Chung D W, Kim Y, Adamczyk L, Garcia R E, Dudney N and Kalinin S V 2010 Nanoscale mapping of ion diffusion in a lithium-ion battery cathode *Nat. Nanotechnol.* **5** 749–54
[8] Gannepalli A, Yablon D G, Tsou A H and Proksch R 2011 Mapping nanoscale elasticity and dissipation using dual frequency contact resonance afm *Nanotechnology* **22** 355705
[9] Garcia R and San Paulo A 1999 Attractive and repulsive tip-sample interaction regimes in tapping-mode atomic force microscopy *Phys. Rev.* B **60** 4961
[10] Agarwal P and Salapaka M V 2009 Real time estimation of equivalent cantilever parameters in tapping mode atomic force microscopy *Appl. Phys. Lett.* **95** 083113
[11] Labuda A, Kocuń M, Meinhold W, Walters D and Proksch R 2016 Generalized hertz model for bimodal nanomechanical mapping *Beilstein J. Nanotechnol.* **7** 970–82
[12] Khalil H K 2002 *Nonlinear Systems* vol 3 (Upper Saddle River: Prentice hall)
[13] Bogoliubov N N 1961 *Asymptotic Methods in the Theory of Non-Linear Oscillations* vol 10 (Delhi: Hindustan Publishing Corporation)
[14] Sebastian A, Gannepalli A and Salapaka M V 2004 The amplitude phase dynamics and fixed points in tapping-mode atomic force microscopy *American Control Conference, 2004. Proceedings of the 2004* **3** 2499–504 IEEE
[15] Sebastian A, Gannepalli A and Salapaka M V 2007 A review of the systems approach to the analysis of dynamic-mode atomic force microscopy *IEEE Trans. Control Syst. Technol.* **15** 952–9
[16] Sanders J A and Verhulst F 1985 *Averaging Methods in Nonlinear Dynamical Systems* volume 59 (New York: Springer)
[17] Cleveland J P, Anczykowski B, Schmid A E and Elings V B 1998 Energy dissipation in tapping-mode atomic force microscopy *Appl. Phys. Lett.* **72** 2613–5
[18] San Paulo A and Garcia R 2002 Unifying theory of tapping-mode atomic-force microscopy *Phys. Rev.* B **66(R)** 041406
[19] Sebastian A, Salapaka M V, Chen D J and Cleveland J P 2001 Harmonic and power balance tools for tapping-mode atomic force microscope *J. Appl. Phys.* **89** 6473
[20] Pintelon R *et al* 1994 Parametric identification of transfer functions in the frequency domain-a survey *IEEE Trans. Autom. Control* **39** 2245–60
[21] Haugstad G 2012 *Atomic Force Microscopy: Understanding Basic Modes and Advanced Applications* (Hoboken, NJ: Wiley)
[22] Sader J E, Sanelli J A, Adamson B D, Monty J P, Wei X, Crawford S A, Friend J R, Marusic I, Mulvaney P and Bieske E J 2012 Spring constant calibration of atomic force microscope cantilevers of arbitrary shape *Rev. Sci. Instrum.* **83** 103705
[23] Salapaka S M, Ramamoorthy A and Salapaka M V 2013 AFM Imaging? Reliable or Not?: Validation and Verification of Images in Atomic Force Microscopy *IEEE Control Systems* **33** 106–18
[24] Ghosal S and Salapaka M 2015 Fidelity imaging for atomic force microscopy *Appl. Phys. Lett.* **106** 013113